Large-Scale Circulation Model for Turbulent Rayleigh-Bénard Convection

Eric Brown and Guenter Ahlers

Department of Physics and iQCD, University of California, Santa Barbara, California 93106, USA

(Received 8 December 2006; published 26 March 2007)

A model for the large-scale-circulation (LSC) of turbulent Rayleigh-Bénard convection in cylindrical samples is presented. It consists of two physically motivated stochastic ordinary differential equations, one each for the strength and the azimuthal orientation of the LSC. Stochastic forces represent phenomenologically the influence of turbulent fluctuations. Consistent with measurements, the model yields an azimuthally meandering LSC with occasional rotations, and with more rare cessations. As in experiment, cessations have a uniform distribution of LSC orientation changes.

DOI: 10.1103/PhysRevLett.98.134501 PACS numbers: 47.27.te, 05.65.+b, 47.27.eb

Rayleigh-Bénard convection (RBC) consists of a fluid-filled container heated from below [1]. Cylindrical containers with aspect ratio $\Gamma \equiv D/L$ (D is the sample diameter and L the height) and $0.5 \lesssim \Gamma \lesssim 3$ have a large-scale circulation (LSC) [2–9] that consists of warm up-flowing and cool down-flowing fluid on opposite sides of the sample. Its near-vertical circulation plane has an orientation θ_0 that undergoes azimuthal diffusion [10–12]. An interesting aspect is that θ_0, in addition to its diffusive meandering, undergoes relatively rapid oscillations that are phase shifted by π at the top relative to the bottom of the sample [8]. In addition, on somewhat longer time scales, the LSC experiences spontaneous and erratic reorientations through an azimuthal displacement $\Delta\theta$ [11–16]. One mechanism for reorientation is a *rotation* of the entire structure without much change of the flow speed [13]. Rotations lead to a power-law distribution of $\Delta\theta$, with small rotations more likely than large ones [11,15]. The other mechanism is a *cessation* of the flow in which it stops briefly and then starts up again in a random new orientation, resulting in a uniform distribution of $\Delta\theta$ [11,15]. Aside from its fundamental interest, the phenomenon of reorientation is important, for instance because it occurs in natural convection of the atmosphere [17], and because cessations of the flow in Earth's outer core are likely to be involved in reversals of Earth's magnetic field [18].

Several models were proposed to reproduce the LSC dynamics. Those of Sreenivasan *et al.* [7] and Benzi [19] were based on similar stochastic equations that were chosen in an attempt to produce the desired reversal events, but they had no way of estimating the parameters and so could not make independent quantitative predictions. The equations yielded two opposite stable flow directions with transitions between them, in qualitative agreement with experiments by Sreenivasan *et al.* [7]. However, such *local* flow reversals usually are not cessations or rotations; they are equivalent to crossings of the LSC orientation past a fixed angle and correspond mostly to small orientation changes, or "jitter" [11]. Another model, by Fontenele Araujo *et al.* [20], was based on a deterministic force balance between buoyancy and drag. It produced LSC reversals ($\Delta\theta = \pi$), but was two dimensional (leaving out the azimuthal coordinate) and so could not reproduce the azimuthal dynamics seen in experiments. Finally, a deterministic model based on the Boussinesq equations with slip boundary conditions and for ellipsoidal sample geometries was developed by Resagk *et al.* [21]. It neglected dissipation and diffusion, but added these effects phenomenologically after the model was derived. The result was a set of ordinary differential equations (ODEs) with several parameters that could be tuned to produce a LSC with various dynamical states, including oscillations (which, however, do not seem to exhibit the phase shift between the top and bottom of the sample [8]) and chaotic meandering; but the existence and statistics of rotations and cessations were not explored.

We present a model consisting of two coupled stochastic ODEs, one for the speed (or "strength") of the LSC and the other for the azimuthal LSC orientation. We retained the physically important terms of the Navier-Stokes (NS) equation and took volume averages. The resulting deterministic ODE for the LSC strength represents the balance between buoyancy and drag forces and has two fixed points; one stable and the other, corresponding to cessations, unstable. The second ODE describes the azimuthal motion of the LSC which is suppressed by its angular momentum. The dynamics of the model arise from the addition of stochastic forces that represent in a phenomenological sense the action of the turbulent fluctuations that exist throughout the system interior. We determined some parameters of the model from independent measurements that did not involve reorientations *per se*, determined others from theory, and did not adjust any of them arbitrarily. In agreement with experiment [11,15], our model yields a few cessations per day with a uniform probability distribution $p(\Delta\theta)$, and more frequent rotations with a power-law distribution.

For the LSC strength we consider the velocity component u_ϕ, where ϕ is an angle that sweeps the plane of the LSC. One expects the acceleration to be due to a balance

between buoyancy and drag forces. Thus we include in the NS equation for u_ϕ only the acceleration, buoyancy, and viscous drag terms, and neglect the nonlinear term [22]:

$$\dot{u}_\phi = g\alpha(T - T_0) + \nu\nabla^2 u_\phi. \quad (1)$$

Here α is the isobaric thermal expansion coefficient, g the acceleration of gravity, and ν the kinematic viscosity.

To obtain an ODE that describes the flow, we take a global average over the field variables that retains the essential physics. For this we use the experimental result [11,12,15,23] that the temperature of the LSC at the side wall at midheight can be written as

$$T = T_0 + \delta\cos(\theta_0 - \theta), \quad (2)$$

where the temperature amplitude $\delta(t)$ represents the strength of the LSC, and where $\theta_0(t)$ is its azimuthal orientation. The buoyancy acts on the entire LSC and is proportional to δ. The profile is taken to be given by Eq. (2), and proportional to the cylindrical radius r. The velocity is assumed to be linear in r and a step function in θ. These assumptions about the flow geometry may affect the coefficients in the equations, but not the functional form. The drag is assumed to occur in the viscous boundary layers of width λ, so $\nabla^2 u_\phi \approx U/\lambda^2$ [$U(t)$ is the maximum speed near the side wall], where $\lambda(t) = (L/2)R_{e,i}^{-1/2}$ [24] ($R_{e,i} \equiv UL/\nu$ is the instantaneous Reynolds number). The volume average requires another factor of $6\lambda/L$ since the drag is mainly in the boundary layers. These approximations result in the volume-averaged [12] equation

$$(2/3)\dot{U} = (2/3\pi)g\alpha\delta - 12\nu^{1/2}U^{3/2}/L^{3/2} \quad (3)$$

which has the steady-state solution

$$(2/3\pi)g\alpha\delta_0 = 12\nu^2 R_e^{3/2}/L^3. \quad (4)$$

Here R_e is the steady-state Reynolds number and δ_0 is the steady-state amplitude. Next we make the assumption that δ is instantaneously proportional to the speed U, since both variables are measures of the LSC strength. The proportionality constant must satisfy Eq. (4). This fixes the proportionality at $(2/3\pi)g\alpha\delta = 12\nu U R_e^{1/2}/L^2$. Equation (4) forces the sum of the powers of U and R_e to be $3/2$. Thus our assumption fixes the powers to be $\delta \propto UR_e^{1/2}$. We substitute this into Eq. (3), combine all parameters into two constants, and add a noise term that represents the turbulent fluctuations of the flow to get the Langevin equation

$$\dot{\delta} = \frac{\delta}{\tau_\delta} - \frac{\delta^{3/2}}{\tau_\delta\sqrt{\delta_0}} + f_\delta(t) \quad (5)$$

with

$$\delta_0 = 18\pi\Delta T\sigma R_e^{3/2}/R; \qquad \tau_\delta = L^2/(18\nu R_e^{1/2}). \quad (6)$$

Here the Rayleigh number is $R \equiv \alpha g\Delta T L^3/\kappa\nu$ with ΔT the applied temperature difference and κ the thermal diffusivity, and the Prandtl number is $\sigma \equiv \nu/\kappa$. In the absence of noise Eq. (5) has two fixed points, one unstable at $\delta = 0$ and one stable when $\delta = \delta_0$. In the stochastic equation this feature reproduces some of the dominating behavior of the LSC which spends most of its time meandering near the stable fixed point at δ_0, but occasionally ceases when fluctuations drive it close to $\delta = 0$.

As an example, we now consider $R = 1.1 \times 10^{10}$, $\sigma = 4.4$, and $\Gamma = 1$ for a sample with $L = 24.76$ cm, $\nu = 6.69 \times 10^{-3}$ cm^2/s, and $\Delta T = 20$ K [25]. Measurements yielded $\delta_0 = 0.25$ K and $R_e = 3700$ [23]. From Eq. (6) one has $\tau_\delta = 85$ s and $\delta_0 = 0.10$ K. For δ_0 theory and experiment are in order-of-magnitude agreement, which is acceptable given the approximations made in the model (for numerical calculations we adopt the experimental value). To learn about the noise intensity, we examined the experimental mean-square amplitude-change $\langle(d\delta)^2\rangle$ ($\langle ... \rangle$ represents a time average) over a time period dt as a function of dt. For time scales that were not too large we found $\langle(d\delta)^2\rangle = D_\delta dt$ with $D_\delta = 3.5 \times 10^{-5}$ K^2/s, suggesting a diffusive process. This method was used before to determine the diffusivity of θ_0 [11,12]; but in the present case the diffusive scaling holds only over intermediate time scales because δ is bounded. With this input we made the noise Brownian with diffusivity D_δ, so $f_\delta(t)$ is Gaussian distributed with width $\sqrt{D_\delta/h}$ where h is the time step in the simulation.

The second Langevin equation describes the azimuthal motion. The driving force is the turbulent noise. The angular-momentum of the LSC in the ϕ coordinate provides a damping force on the azimuthal motion. This phenomenon is represented by the transport term in the NS equation. We show below that the viscous drag across the boundary layer near the side wall is small compared to this transport term. Thus, for now neglecting the drag term (and Earth's Coriolis force; see [12]), we have

$$\dot{u}_\theta + (\vec{u}\cdot\vec{\nabla})u_\theta = 0. \quad (7)$$

A volume average gives $(1/3)L\ddot{\theta}_0 = -(2/3)U\dot{\theta}_0$. The viscous drag can be approximated by $\dot{u}_{\theta,drag} = -6\nu R_e^{1/2}\dot{\theta}_0/L$ (Ref. [12], Eq. 10). Thus its ratio to that of the angular-momentum damping is equal to $9R_e^{-1/2} \approx 0.15$ for $R_e = 3700$, justifying its neglect. One sees that the angular-momentum leads to a variable damping that is proportional to the LSC strength U. Again we convert U to δ, combine the remaining parameters to get a new constant, and add a noise term representing turbulent fluctuations to get

$$\ddot{\theta}_0 = -\frac{\dot{\theta}_0\delta}{\tau_{\dot\theta}\delta_0} + f_{\dot\theta}(t); \qquad \tau_{\dot\theta} = \frac{L^2}{2\nu R_e}. \quad (8)$$

For our example $\tau_{\dot\theta} \simeq 13$ s. The turbulent noise in this coordinate is also found to be Brownian, with diffusivity $D_{\dot\theta} = 2.5 \times 10^{-5}$ rad^2/s^3. This diffusivity comes from a fit of $\langle(d\dot{\theta}_0)^2\rangle = D_{\dot\theta}dt$ to experimental data, where $\langle(d\dot{\theta}_0)^2\rangle$ is the mean-square change in rotation rate over the time period dt. This scaling also only holds for short time periods because $\dot{\theta}_0$ is bounded.

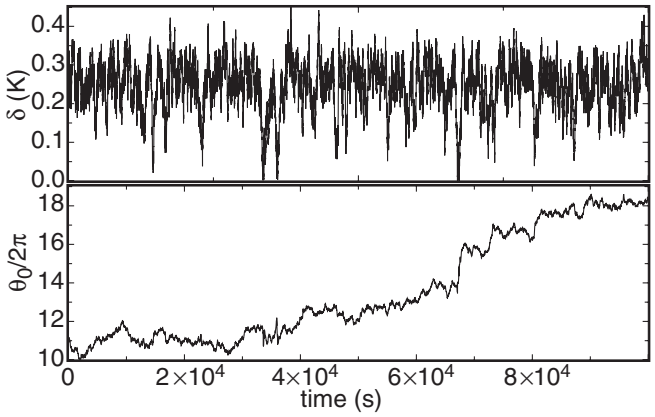

FIG. 1. Time series of δ and θ_0 from the simulation of Eqs. (5) and (8). δ fluctuates around δ_0, and occasionally those fluctuations are large enough to cause a cessation where $\delta \approx 0$.

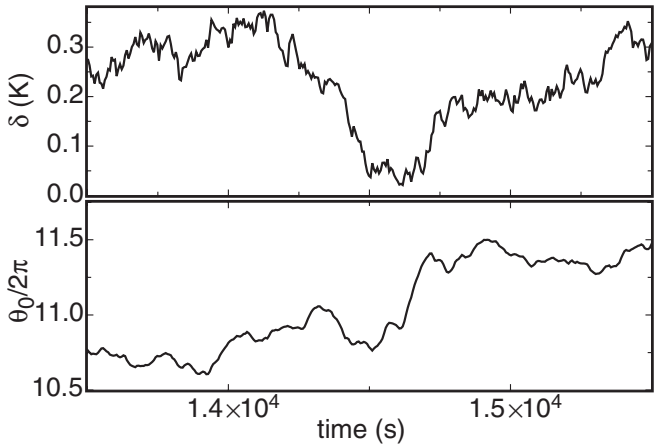

FIG. 2. Short section of the time series from Fig. 1 showing a cessation. δ drops to near zero; while δ is small, the azimuthal motion becomes fast because it is no longer suppressed by the LSC angular momentum.

The two stochastic ODEs Eqs. (5) and (8) are our model for the LSC dynamics. Using the experimentally determined values of δ_0, D_δ, and $D_{\dot\theta}$, and the predictions of Eqs. (6) and (8) for τ_δ and $\tau_{\dot\theta}$ with the measured value of R_e, they can be integrated numerically to get time series for δ and θ_0 as shown in Fig. 1 over about 1 day. One can see, as we expected, that the LSC amplitude δ is stable with an occasional cessation where the amplitude drops to zero. From much longer simulations we found that cessations occur about 3.8 times per day, which is about twice the frequency measured experimentally [11], a good agreement considering the approximations of the model. Figure 1 shows that the orientation meanders as expected, but one must look on a shorter time scale to see the details of the dynamics. Thus, Fig. 2 shows a shorter section of the same time series that contains a cessation. One sees how δ gradually drops to zero, then grows back up again over a few hundred seconds, just as observed experimentally [11]. The time series for θ_0 contains a large change in θ_0 during the cessation, which is also seen in experiments [11]. Equation (8) for the azimuthal motion implies that, when δ and thus the angular momentum are small during cessations, the damping term becomes small so the turbulent fluctuations are free to accelerate the LSC to large azimuthal rotation rates. When the LSC is strong, i.e., $\delta \approx \delta_0$, then the larger angular momentum of the LSC suppresses the azimuthal rotation. This inverse relationship between δ and $\dot\theta_0$ was observed in experiments [11,15] but had not been explained by any previous model.

To determine the statistics of cessations and rotations, we analyzed the simulated time series using the same algorithms as those applied before to experimental data [11,15]. Figure 3(a) shows the probability distribution $p(\Delta\theta)$ of the orientation change $\Delta\theta$ during cessations. The results from the simulations are consistent with a uniform distribution $p(\Delta\theta) = 1/\pi$, in agreement with the experiments [11,15]. This is an important result that no model had predicted before, either because the model was attempting to describe a reversal of the flow direction, i.e., $\Delta\theta = \pi$ and the θ dependence was not contained in it [7,19,20], or because the issue was not addressed [21]. The angular momentum that usually suppresses the azimuthal motion of the LSC is reduced during cessations, allowing turbulent fluctuations to azimuthally rotate the LSC freely. For large enough noise strengths, the azimuthal distance traveled is large over the duration of the cessation, and this results in a final orientation independent of the orientation before the cessation, which explains the uniform $p(\Delta\theta)$. We also find rotations in the model to result from a similar mechanism. Rotations typically occur when the angular momentum of the LSC is still large, so the azimuthal rotation is limited. This results in a monotonically decreasing distribution of $\Delta\theta$ for rotations. However, the azimuthal rotation rate can become large even when δ is somewhat lower than normal, resulting in more rotations, and, in particular, more large rotations, than would be

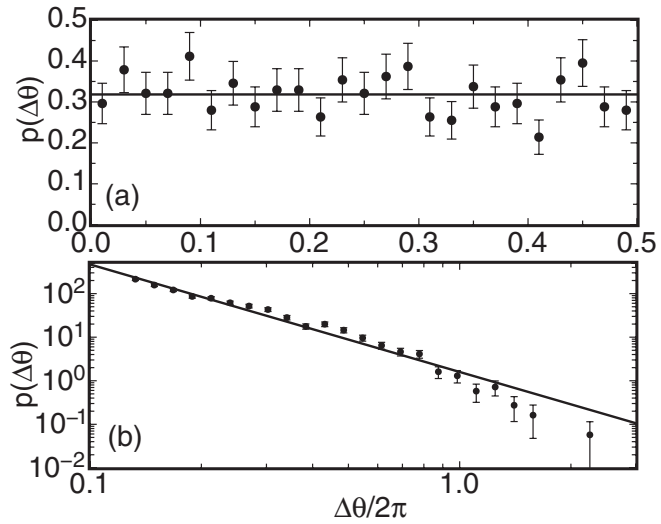

FIG. 3. (a) Probability distribution of the azimuthal change $\Delta\theta$ during cessations. Solid line: the uniform distribution $p(\Delta\theta) = 1/\pi$. (b) $p(\Delta\theta)$ for rotations. Solid line: a power-law fit.

expected from purely Brownian noise with constant damping coefficient, a conclusion which was also implied by experiments [11]. The simulation results can be represented reasonably well by a power law for $p(\Delta\theta)$ as shown in Fig. 3(b), with an exponent of -2.5 in qualitative agreement with the experiments [15], which gave a power law with an exponent of -3.8. The significance of this exponent is unknown to us. The rate of reorientations is 5 times larger in the simulation than in the experiment, which is in order-of-magnitude agreement. In the simulation, successive cessations and reorientations are found to be independent of each other, i.e., the time intervals between events are Poisson distributed, in agreement with the measurements [11,15].

We derived a dynamical model, motivated by the Navier-Stokes equations, to describe the large-scale circulation in cylindrical samples of aspect ratio Γ between 0.5 and 3 where a single convection roll is expected. The model contains two variables: the LSC strength δ and azimuthal orientation θ_0. It uses as input four parameters that were determined, for the example $\Gamma = 1$, from independent experimental measurements; it requires no tunable parameters. Equation (5) for δ differs from the equations of Refs. [7,19] in that the nonlinearity is of order $3/2$ rather than of the more usual cubic order, although this does not qualitatively change the flow dynamics. The major improvements over those models are the physical motivation of the equations, and the additional equation for azimuthal motion, including the angular-momentum term which provides a relationship between the wind strength and azimuthal dynamics. The model produces a stable LSC with occasional cessations and rotations that have properties similar to those found in experiments. The azimuthal dynamics during cessations can be understood in terms of the angular momentum of the LSC which suppresses azimuthal motion driven by turbulent fluctuations. An in-phase oscillation of frequency ω predicted by [21] is not contained in the model, but could be reproduced by adding a restoring-force term $-\omega^2\theta_0$ to Eq. (8). In cylindrical containers we see no physical reason to do this, but such a term would arise from the modified pressure field due to a slightly noncircular container. Our two-dimensional model of course will not predict the three-dimensional twisting oscillations of the LSC [8], which would require an additional degree of freedom and a restoring force presumably related to momentum transport. The model can, however, be used to predict the dependence on R of the LSC parameters, LSC dynamics in RBC samples that are tilted relative to gravity [23], or in samples of weakly broken rotational invariance [12], and the influence of Earth's Coriolis force on the LSC [12]; these issues are to be studied thoroughly in future work.

In a broader sense, we have shown an example where turbulent fluid-flow dynamics can be described by physically motivated ordinary differential equations with stochastic terms that represent the turbulent background fluctuations. This modeling process should be applicable to other turbulent flow problems, although different physical terms may be necessary.

We benefited from conversations with numerous colleagues, especially with Detlef Lohse. This work was supported by the National Science Foundation through Grant No. DMR07-02111.

[1] E. Siggia, Annu. Rev. Fluid Mech. **26**, 137 (1994); L. Kadanoff, Phys. Today **54**, No. 8, 34 (2001); G. Ahlers, S. Grossman, and D. Lohse, Physik J. **1**, 31 (2002).
[2] For instance, R. Krishnamurti and L. N. Howard, Proc. Natl. Acad. Sci. U.S.A. **78**, 1981 (1981).
[3] M. Sano, X.-Z. Wu, and A. Libchaber, Phys. Rev. A **40**, 6421 (1989).
[4] B. Castaing, G. Gunaratne, F. Heslot, L. Kadanoff, A. Libchaber, S. Thomae, X.-Z. Wu, S. Zaleski, and G. Zanetti, J. Fluid Mech. **204**, 1 (1989).
[5] S. Ciliberto, S. Cioni, and C. Laroche, Phys. Rev. E **54**, R5901 (1996).
[6] X.-L. Qiu and P. Tong, Phys. Rev. E **64**, 036304 (2001).
[7] K. R. Sreenivasan, A. Bershadskii, and J. J. Niemela, Phys. Rev. E **65**, 056306 (2002).
[8] D. Funfschilling and G. Ahlers, Phys. Rev. Lett. **92**, 194502 (2004).
[9] Y. Tsuji, T. Mizuno, T. Mashiko, and M. Sano, Phys. Rev. Lett. **94**, 034501 (2005).
[10] C. Sun, H.-D. Xi, and K.-Q. Xia, Phys. Rev. Lett. **95**, 074502 (2005).
[11] E. Brown and G. Ahlers, J. Fluid Mech. **568**, 351 (2006).
[12] E. Brown and G. Ahlers, Phys. Fluids **18**, 125108 (2006).
[13] S. Cioni, S. Ciliberto, and J. Sommeria, J. Fluid Mech. **335**, 111 (1997).
[14] J. J. Niemela, L. Skrbek, K. R. Sreenivasan, and R. J. Donnelly, J. Fluid Mech. **449**, 169 (2001).
[15] E. Brown, A. Nikolaenko, and G. Ahlers, Phys. Rev. Lett. **95**, 084503 (2005).
[16] H.-D. Xi, Q. Zhou, and K.-Q. Xia, Phys. Rev. E **73**, 056312 (2006).
[17] E. van Doorn, B. Dhruva, K. R. Sreenivasan, and V. Cassella, Phys. Fluids **12**, 1529 (2000).
[18] G. Glatzmeier, R. Coe, L. Hongre, and P. Roberts, Nature (London) **401**, 885 (1999).
[19] R. Benzi, Phys. Rev. Lett. **95**, 024502 (2005).
[20] F. Fontenele Araujo, S. Grossmann, and D. Lohse, Phys. Rev. Lett. **95**, 084502 (2005).
[21] C. Resagk, R. du Puits, A. Thess, F. V. Dolzhansky, S. Grossmann, F. Fontenele Araujo, and D. Lohse, Phys. Fluids **18**, 095105 (2006).
[22] In the absence of azimuthal motion the nonlinear term cancels in the volume average to be taken below. Its contribution may be neglected because the azimuthal motion is slow compared to u_ϕ.
[23] G. Ahlers, E. Brown, and A. Nikolaenko, J. Fluid Mech. **557**, 347 (2006).
[24] See, for instance, S. Grossmann and D. Lohse, Phys. Rev. E **66**, 016305 (2002).
[25] E. Brown, A. Nikolaenko, D. Funfschilling, and G. Ahlers, Phys. Fluids **17**, 075108 (2005).